

Interatomic Coulombic decay of a Li dimer in a coupled electron and nuclear dynamics approachR. Cabrera-Trujillo ^{1,2,*}, O. Vendrell ² and L. S. Cederbaum²¹*Instituto de Ciencias Físicas, Universidad Nacional Autónoma de México, Avenida Universidad S/N, Colonia Chamilpa, Cuernavaca, Morelos 62210, Mexico*²*Theoretische Chemie, Physikalisch-Chemisches Institut, Universität Heidelberg, INF 229, 69120 Heidelberg, Germany*

(Received 16 July 2020; accepted 3 September 2020; published 28 September 2020)

Interatomic Coulombic decay (ICD) is a fundamental process between atoms or molecules via a neighbor interaction that produces a relaxation of an electronically excited atom or molecule when embedded in an environment. Due to the physical nature of the process, the electronic and nuclear degrees of freedom are coupled. In this paper, we study the ICD process for a lithium dimer by means of the electron and nuclear dynamics (END) approach. The END approach incorporates a full time-dependent description of the electronic and nuclear degrees of freedom, although its current version does not properly account for continuum states and has limitations in the electronic description by using a single determinantal wave function. Despite this, we confirm that the ICD process takes place via a dipole interaction that induces the nuclear motion of the dimer with a consequent electronic population transfer to higher excited states simulating the ionization process. When the dimer approaches a distance of around 11.5 a.u. (6 Å), this ionization process takes place due to the dipole coupling and occurs at the place of the strongest attractive dipole force. Passing that point, we find that the two lithium atoms repel each other via a Coulomb explosion process followed with a consequent kinetic-energy release (KER). We determine the KER and the timing of the ICD process. We point out the strengths and weaknesses of the END approach and the required enhancements to account for a better description of the ICD process in a coupled electron and nuclear dynamics.

DOI: [10.1103/PhysRevA.102.032820](https://doi.org/10.1103/PhysRevA.102.032820)**I. INTRODUCTION**

The interaction of atoms with the environment is known to cause distortions in the atom or molecule electronic structure with effects in the broadening of spectral lines as well as in the decay process. One of the authors [1] has predicted that if an excited atom or molecule is put in the neighborhood of another atom or molecule a mechanism occurs called interatomic Coulombic decay (ICD). The excited system can transfer its energy in an extremely efficient way to a neighboring system which then releases that energy by emission of one of its own outer-shell electrons. ICD is different from the Auger decay since the electron cannot emerge from the excited system itself, but is ejected from its neighbor's valence shell. Furthermore, this emission is not mediated by the overlap of the participating wave functions but rather by an energy transfer via a virtual photon. Since its theoretical prediction, it has been observed experimentally in van der Waals clusters [2–6], in hydrogen bonded systems [6–8], in He dimers at very large distance [9], after Auger and resonant Auger processes [10–13], and after ionization of a water molecule in water clusters [6,8]. From here on, the term “dimer” is used for two atoms in gas phase that are not bound, but nearby. Recently, ICD has been predicted also to occur from vibrational to electronic degrees of freedom [14]. Furthermore, ICD has been observed in nanosystems, e.g., in

a pair of singly charged noncoupled semiconductor quantum dots (QDs) [15,16]. Here, ICD has been predicted to be the dominant decay channel of a two-electron Feshbach resonance state delocalized over two QDs. Recently, laser-induced ICD in QDs with electron dynamics at a multiconfigurational time-dependent Hartree-Fock level have been reported for a two-dimensional continuum, such that ICD control with laser polarization is technologically achievable [17]. Very recently, Agueny *et al.* [18] have predicted enhanced energy transfer via bridge assisted mechanisms for ICD in coupled QDs.

There exist several theoretical approaches to study ICD processes. One approach consists in calculating the rates using an *ab initio* calculation of interatomic decay rates by a combination of the Fano ansatz, Green's-function methods, and Stieltjes imaging technique [19] and extensions thereof like the Fano-Stieltjes method applied to Lanczos pseudospectra [20]. Another approach relies on the Hamiltonian continued into the complex energy plane [21–25]. The decaying states become resonances with complex energies, where the imaginary part is related to the inverse lifetime.

In the above methods, the ICD rates are calculated at fixed values of the interatomic (intermolecular) distances and the nuclear dynamics of the ICD is calculated afterwards using the resulting complex potential-energy surfaces [26–28]. We propose to use a different theoretical approach based on an *ab initio* time-dependent solution of the Schrödinger equation that incorporates electronic and nuclear coupling, the so-called electron and nuclear dynamics (END) [29]. Although the current version of END does not account properly for the

*Corresponding author: trujillo@icf.unam.mx

electronic continuum and it is limited to a single determinant, the coupled electron and nuclei dynamics induced by the dipole interaction accounts for the ICD process. END has successfully been applied in atomic and molecular collisions [30–32], charge exchange [32–34], molecular fragmentation [35,36], and energy-loss processes [31,37].

In Sec. II A, we present a review of the ICD main assumptions while in Sec. II B a summary of the electron and nuclear dynamics approach, as implemented to the study of the interatomic Coulombic decay, is provided. Our results and discussion are presented in Sec. III and our conclusions are given in Sec. IV.

II. THEORY

A. ICD assumptions

Let us consider two atomic or molecular systems denoted as A and B , separated by a distance R . The rate of the ICD relaxation process is determined by Fermi's "golden rule":

$$\Gamma = 2\pi \sum_f |(\Psi_i|V|\Psi_f)|^2 \quad (1)$$

where V is the interaction between system A and its neighbor B . We shall concentrate here, for simplicity of presentation, on large distances between A and B and only mention that ICD is highly operative at typical distances between atomic and molecular systems. The wave functions Ψ_i and Ψ_f describe the initial and final states of the process in the absence of this interaction. The initial state is given by the product $\Psi_i = \phi_i^A \phi_i^B$ and the final state is given by $\Psi_f = \phi_f^A \phi_f^B$, where ϕ_i^j is the atomic or molecular wave function of system j . Let the electronic and nuclear coordinates of system A , relative to its center of mass, be \mathbf{r}_i and \mathbf{R}_k and let those of system B , relative to its center of mass, be \mathbf{r}'_j and \mathbf{R}'_j . Expanding the interaction V in inverse powers of the distance between the two centers of mass, R , provides the leading contributing term [38]:

$$V \approx \frac{-3(\hat{\mathbf{u}} \cdot \mathbf{D}^A)(\hat{\mathbf{u}} \cdot \mathbf{D}^B) + \mathbf{D}^A \cdot \mathbf{D}^B}{R^3} \quad (2)$$

where $\hat{\mathbf{u}}$ is the unit vector connecting the two centers of mass, and $\mathbf{D} = -\sum_i \mathbf{r}_i + \sum_k Z_k \mathbf{R}_k$ is the dipole operator of system A with a similar expression for system B . Here Z_k indicates the nuclear charges. Averaging over the orientations of the system and its neighbor leads to

$$\Gamma = \frac{4\pi}{3R^6} \sum_f |\mathbf{D}_{i,f}^A|^2 |\mathbf{D}_{i,f}^B|^2 \quad (3)$$

where $\mathbf{D}_{i,f}^A = \langle \phi_i^A | \mathbf{D}^A | \phi_f^A \rangle$ is the transition dipole moment of system A and with a similar expression for system B .

We can view the process presented above as follows. The neighbor subsystem B achieves an excess energy through excitation by a photon or by the impact with another particle. This excess energy may be in the form of an electronic excitation or an electron hole state in a shell other than the outermost valence orbital [39]. This electron hole or excitation is not stable but, crucially, the excess energy is not sufficient for an autoionization process at subsystem B to occur. This excess energy can either be carried away from subsystem B

by emission of an extreme UV or x-ray fluorescence photon or transferred via Coulomb forces to subsystem A , in which an electron subsequently escapes from the atomic binding. When possible energetically, the latter nonradiative mechanism of deexcitation is extremely efficient in comparison to the competing photon emission [40]. Indeed, the characteristic times are typically less than 100 fs (1 fs = 10^{-15} s) to even less than 1 fs [41] entering the attosecond regime (1 as = 10^{-18} s), compared to radiative decay lifetimes, which, except for core levels of heavy elements, belong to the nanosecond range (1 ns = 10^{-9} s). Equation (3) implies that systems with large allowed transition dipole moments will have a large ICD rate. Furthermore, the process depicted before assumes two static systems A and B separated initially by a distance R_0 . In order to have a time-dependent description of the ICD process, it is required to solve the time-dependent Schrödinger equation where the decay width, as a function of nuclear coordinates, serves as the imaginary part of the complex potential surfaces involved.

B. Electron and nuclear dynamics approach

For the study of the interatomic Coulomb decay, we use a nonadiabatic approach that takes into account the electronic and nuclear coupling within the time-dependent variational principle (TDVP) to solve the time-dependent Schrödinger equation. This method is called the END. As the details of the END method have been reported elsewhere [29], we present here only a brief summary of the theory.

The simplest level of the END theory employs a wave function

$$|\psi\rangle = |z, \mathbf{R}, \mathbf{P}\rangle |\mathbf{R}, \mathbf{P}\rangle = |z\rangle |\phi\rangle \quad (4)$$

where

$$|\mathbf{R}, \mathbf{P}\rangle = \prod_k \exp \left[-\frac{1}{2} \left(\frac{\mathbf{X}_k - \mathbf{R}_k}{\omega_k} \right)^2 + i\mathbf{P}_k \cdot (\mathbf{X}_k - \mathbf{R}_k) \right] \quad (5)$$

is the nuclear wave function with \mathbf{R}_k and \mathbf{P}_k denoting the average position and momentum of a nucleus, respectively, and where

$$|z, \mathbf{R}, \mathbf{P}\rangle = |z\rangle = \det\{\chi_i(x_j, \mathbf{R}, \mathbf{P})\} \quad (6)$$

is a complex, spin unrestricted, electronic single determinantal wave function, which is built from dynamical molecular spin orbitals:

$$\chi_i = \phi_i + \sum_{j=N+1}^K \phi_j z_{ji}, \quad i = 1, 2, \dots, N. \quad (7)$$

Here, N is the number of electrons and K is the states generated by the electronic basis set. These molecular spin orbitals are expressed as a linear combination of atomic spin orbitals formed from Gaussians centered on the average nuclear position, \mathbf{R}_k , of the dynamically moving nuclei with momentum \mathbf{P}_k through electron-translation factors [29]. Forming the quantum-mechanical Lagrangian, in the limit of zero width parameters $\{\omega_k\}$ and using the TDVP, produces a set of dynamical equations that govern the time evolution of the dynamical variables $\{z, \mathbf{R}, \mathbf{P}\}$. It is important to note that the dynamics of the system is treated in a laboratory Cartesian

system of coordinates, thus circumventing the problem of choosing internal coordinates. The fact that the overall translation and rotational degrees of freedom are included causes no problem since the dynamical equations satisfy general total linear and angular momentum invariance properties [29].

The resulting END dynamical equations are expressed in matrix form as [29]

$$\begin{pmatrix} 0 & -i\mathbf{C}^* & -i\mathbf{C}_R & -i\mathbf{C}_P^* \\ i\mathbf{C} & 0 & -i\mathbf{C}_R^* & i\mathbf{C}_P \\ i\mathbf{C}_R^\dagger & -i\mathbf{C}_R^T & \mathbf{C}_{RR} & -\mathbf{I} + \mathbf{C}_{RP} \\ i\mathbf{C}_P^\dagger & -i\mathbf{C}_P^T & \mathbf{I} + \mathbf{C}_{RP} & \mathbf{C}_{PP} \end{pmatrix} \begin{pmatrix} \dot{\mathbf{z}} \\ \dot{\mathbf{z}}^* \\ \dot{\mathbf{R}} \\ \dot{\mathbf{P}} \end{pmatrix} = \begin{pmatrix} \partial E / \partial \mathbf{z} \\ \partial E / \partial \mathbf{z}^* \\ \partial E / \partial \mathbf{R} \\ \partial E / \partial \mathbf{P} \end{pmatrix}. \quad (8)$$

Here $\dot{\mathbf{z}} = d\mathbf{z}/dt$ and $E = \sum_l P_l^2/2M_l + \langle \mathbf{z}, \mathbf{R}, \mathbf{P} | H_{el} | \mathbf{z}, \mathbf{R}, \mathbf{P} \rangle$ is the total energy of the system with M_l the nuclear mass and H_{el} the electronic Hamiltonian including the nuclear-nuclear repulsion term. The nonadiabatic coupling terms between electrons and nuclei are expressed in terms of the elements of the dynamical metric as

$$C_{ph;qg} = \left. \frac{\partial^2 \ln S(z^*, R, P, z, R', P')}{\partial z_{ph}^* \partial z_{qg}} \right|_{R'=R, P'=P},$$

$$(C_{X_{ik}})_{ph} = \left. \frac{\partial^2 \ln S(z^*, R, P, z, R', P')}{\partial z_{ph}^* \partial X_{ik}} \right|_{R'=R, P'=P},$$

$$(C_{XY})_{ij;kl} = -2 \operatorname{Im} \left. \frac{\partial^2 \ln S(z^*, R, P, z, R', P')}{\partial X_{ij} \partial Y_{kl}} \right|_{R'=R, P'=P},$$

which are defined in terms of the overlap $S = \langle \mathbf{z}, R, P | \mathbf{z}, R', P' \rangle$ of the determinantal states of two different nuclear configurations. In Eq. (8), the detailed coupling of the electronic and nuclear degrees of freedom is clearly discernible. This, the simplest of END approximations, can be labeled time-dependent Hartree-Fock for electrons and narrow wave-packet nuclei. This approximation has been implemented in the ENDYNE code [42].

For the study of the Li dimer ICD process, we require the specification of initial conditions of the system under consideration. Initially, a Li($1s^2 2s$) atom is placed at the origin (system A) while a second Li⁺($1s 2s$) ion (system B) is placed at an initial distance R_0 , on the z axis, with both of them having zero initial momentum (at rest). In Fig. 1, we show a sketch of the initial configuration of the system and how the ICD process takes place. Notice that one $1s$ electron from atom B has been removed to become the excited neighbor. The initial dimer separation, R_0 , ranges from 12 to 40 a.u. in steps of 4 a.u. corresponding to 5 to 18 Å in steps of 1.8 Å. The time evolution is finished when the two systems are well separated. This time is up to 400 000 a.u. or 9.7 ps. To ensure converged results, the adaptive differential equation solver uses a maximum $\Delta t \approx 10^{-4}$. At each time step, ENDYNE calculates all the one- and two-electron integrals, such that the dynamics

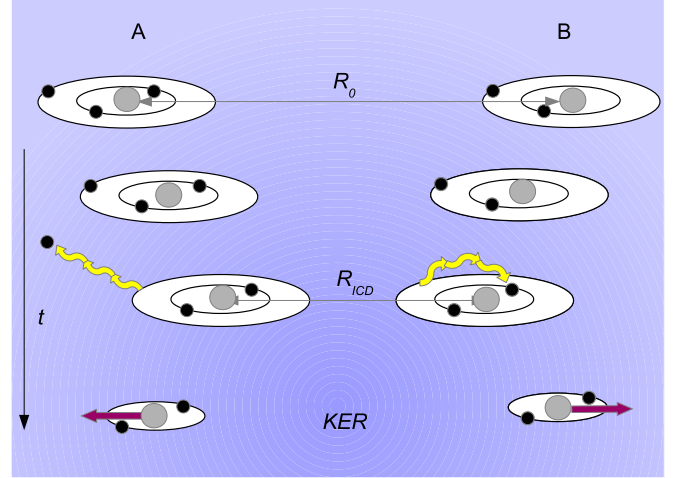


FIG. 1. Sketch of the Li dimer ICD process. Initially the dimer is separated a distance R_0 with the atom B being the ion (a $1s$ electron has been removed) and atom A being the neutral atom (neighbor). As time passes, the dipole interaction causes them to attract and the ICD process occurs at a critical distance R_{ICD} where they decelerate and then the Coulomb repulsion occurs with a kinetic-energy release (KER).

takes between one and three weeks in a 3.2-GHz computer for each initial separation. For our paper, we tested several bases sets, ranging from STO-3G, to 3-21G (and all the polarization branches), up to aug-cc-pVTZ [43]. This last one took too long to really consider it as a good candidate to study ICD. We found that the aug-cc-pVDZ [$10s5p2d/4s3p2d$] with two even-tempered [44,45] diffuse s and p orbitals basis set described better the dynamics with a good compromise between calculation time and the description of the dynamics. We estimate the error in our calculations by adding one or two extra diffuse orbitals to the basis set. This extended the calculation time from ten days to three weeks. We found no noticeable changes (less than 1%) in any of the properties of interest (momentum, excited-state populations, charge dynamics).

Once the wave function is determined at the end of the time evolution, the electron-excitation and interatomic Coulombic decay probability, as a function of the time t and initial atom separation R_0 , is obtained by performing a projection of the atomic n th state as

$$P_n(t, R_0) = |\langle \Phi_n | \Psi(t, R_0) \rangle|^2, \quad (9)$$

where Φ_n is the final excited state of the Li atom of interest and Ψ is the final evolved molecular wave function.

III. RESULTS AND DISCUSSION

A. Position and momentum dynamics

In Fig. 2(a), we show the distance between the two lithium atoms, $R(t)$, as a function of time. Due to the induced dipole moment between the Li⁺ ion and the Li atom, the initial motion is attractive. In all the cases, we observe that the closest distance of approach is around 7 a.u. (3 Å), which occurs at time t_{\min} . However, the electronic transition of the $2s$ electron into higher excitation and ionization states of the neutral atom occurs at an earlier time, marked by an

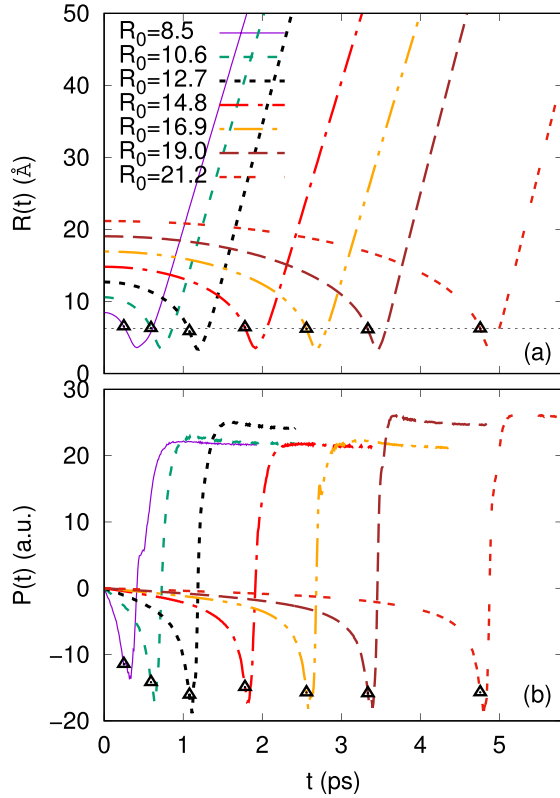


FIG. 2. (a) Li dimer relative distance, $R(t)$, as a function of time for several initial distances R_0 . The open triangle symbols and the dashed line that horizontally joins them denote the positions at which the ICD $2s$ electron from atom A is promoted to higher excited states (see Fig. 3). (b) Li dimer relative momentum, $P(t)$, as a function of time. The open triangle symbols denote when the ICD excitation and ionization occur. Notice that initially the ion and atom attract each other and then after the ICD has taken place they repel each other. The time of closest approach occurs when $P(t_{\min}) = 0$.

open triangle symbol, corresponding to a larger distance of 11.5 a.u. or 6 Å. For all studied initial conditions, the ICD process occurs at this distance before arriving at the distance of closest approach. We label this distance R_{ICD} , which occurs at a time t_0 from the beginning of the dynamics. The energy-transfer process produces a highly excited Li^* atom with the valence electron being excited and ionized to a very diffuse orbital. Owing to the large delocalization of the ICD electron in the finite basis of the Li^* system, the two subsystems experience a strong Coulomb repulsion and repel in a Coulomb explosion process. One observes that ICD occurs just at the onset of the closest approach. As the basis set does not properly describe the ionization channel into a true continuum, the two atoms separate with constant relative velocity after they have reached a distance beyond the outermost diffuse orbitals in the Li^* atom, as observed from the constant slope of the curve $R(t)$.

In Fig. 2(b), we show the relative momentum between the two atoms as a function of time. We observe first an accelerated attractive interaction as expected by the dipole interaction of the dimer. Then the attraction stops followed by a repulsion that occurs at the onset of the excitation and ionization of the $2s$ electron of the neutral lithium atom. The

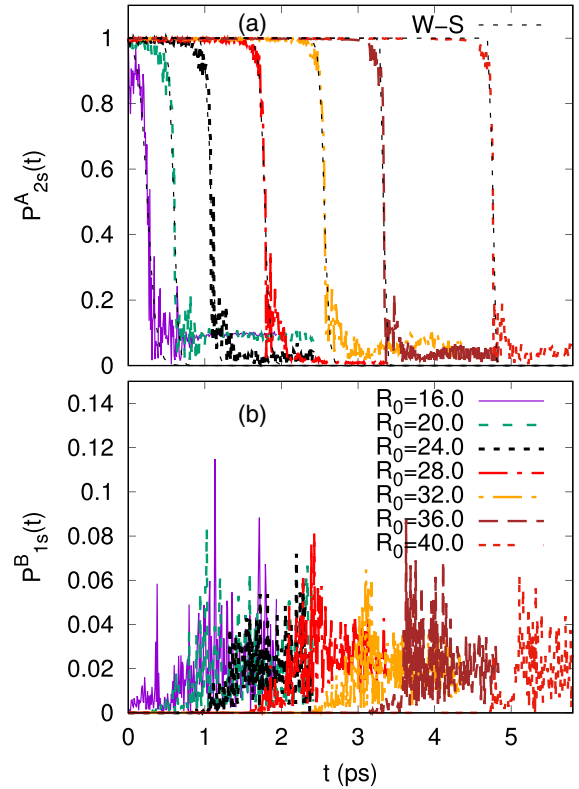


FIG. 3. (a) Probability to find the valence electron of the system A lithium in its $2s$ state as a function of time for several relative initial distances R_0 . The dashed line represents the Woods-Saxon function that fits the excitation process. Notice that in the ICD process the $2s$ orbital of the initially neutral atom is emptied at a time t_0 with a width δ . (b) Probability to find an electron in the $1s$ core orbital of the system B lithium as a function of time.

onset of the excitation and ionization is marked by the open triangle symbols. Notice that this point corresponds to the largest slope in the $P(t)$ curve, i.e., largest force. After the ICD has occurred, the relative momentum becomes constant, i.e., the atoms separate with a constant velocity after the onset of the simulated ICD process.

B. ICD electronic population

In Fig. 3(a), we show the probability for finding the valence electron of the neutral lithium atom, system A , in the $2s$ state as a function of time. We observe that the onset of the excitation and ionization occurs in a well-defined time, leaving the $2s$ orbital unoccupied. This is the time t_0 mentioned previously. We notice that the $2s$ population, as a function of time, follows a Wood-Saxon function:

$$P(t) = \frac{1}{1 + e^{(t-t_0)/\delta}}, \quad (10)$$

where t_0 is the time for the onset of the ICD decay, which corresponds to a distance R_{ICD} , and δ is the width for the decay or diffuseness of the ICD process. In Table I, we provide the values for t_0 and δ , as well as the distance R_{ICD} and the minimal distance reached by the dimer, R_{\min} for each initial distance R_0 of the dynamics.

TABLE I. Parameters for the ICD onset, as obtained from the Woods-Saxon function, Eq. (10), when adjusted to the END results. R_0 is the initial separation of the Li dimer; t_{\min} is the time from the beginning of the dynamics to the closest approach of the dimer, R_{\min} . t_0 is the onset of the ICD which occurs as a separation R_{ICD} and δ is the width of the decay.

R_0 (Å)	t_{\min} (ps)	R_{\min} (Å)	t_0 (ps)	δ (fs)	R_{ICD} (Å)
8.5	0.414	3.598	0.249	57.0	6.530
10.6	0.728	3.466	0.593	28.0	6.303
12.7	1.187	3.323	1.079	30.0	5.863
14.8	1.913	3.530	1.781	34.0	6.398
16.9	2.684	3.149	2.560	30.0	6.207
19.1	3.457	3.164	3.337	12.0	6.117
21.2	4.876	3.191	4.758	13.0	6.234

In Fig. 3(b), we show the probability of finding the relaxing electron in the $1s$ state of the lithium ion, system B , as a function of time. We observe that during the onset of the excitation and ionization the probability of finding an electron in the $1s$ shell of lithium increases, but it is still too small compared to what is expected in a complete ICD process where this state should be filled. The reason is that in a static one determinantal description two electron excitations and correlation effects are missing, so there is no mechanism to make the electron deexcite nonradiatively into the inner shell. However, END still captures properly the physical process due to the time-dependent dynamics of electrons and nuclei.

C. Potential-energy curves

The previous conclusions are reinforced by analyzing the potential-energy curves (PECs) of the $\text{Li}(1s^22s) + \text{Li}^+(1s2s)$ system as a function of the initial separation R_0 . In Fig. 4(a), we show the PECs as obtained at the Hartree-Fock level of theory, as the results of the eigenvalues of the mean-field Fock operator, for the excitations of the dimer as a function of the dimer separation R_0 . We recall that initially the system starts the interaction in the curve labeled $\text{Li}(1s^22s) + \text{Li}^+(1s2s)$. The ion and atom start to approach each other due to the dipole interaction until they reach a distance of approximately 11.5 a.u. (6 Å) where the maximum of the dipole transition moment is reached and the electronic transition occurs for the $2s$ electron towards the $2p$ state and further up. This is observed in Fig. 4(b) where we show the transition dipole moment between the $\text{Li}(1s^22s) + \text{Li}^+(1s2s)$ and the $\text{Li}(1s^22p) + \text{Li}^+(1s2s)$ state of the dimer as a function of the separation R_0 , as obtained at the Hartree-Fock level of theory. Notice that the largest transition dipole moment is at $R_0 \sim 6.5$ Å, which corresponds to R_{ICD} for the ICD process. As the process continues, energy is transferred to atom A , generating a pseudoionized $\text{Li}^*(1s^2)$. This occurs because of the lack of a proper description of the continuum by the END approach, which forces the electron to occupy a very diffuse pseudocontinuum state. The second lithium ion B is found within this diffuse electron cloud and sees therefore a positive charge at the center of the pseudoionized atom, such that Coulombic repulsion takes place, as we have sketched in Fig. 1 and observed in Fig. 2. This Coulombic explosion

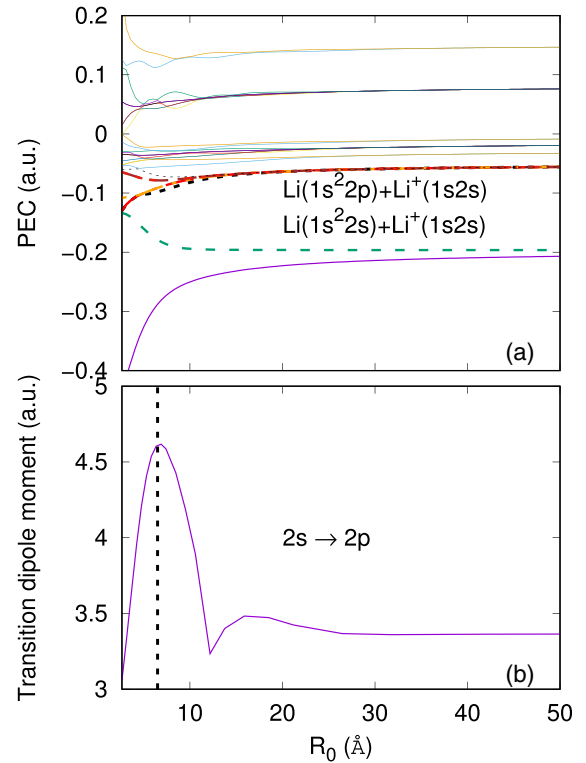


FIG. 4. (a) Potential-energy curves (PECs) for the $\text{Li}^+ + \text{Li}$ dimer as a function of the relative distance, R_0 , as obtained at the Hartree-Fock level. The initial potential-energy curve is shown as a (green) broken line and carries the label $\text{Li}^+(1s2s) + \text{Li}(1s^22s)$. (b) Transition dipole moment (coupling term) between the initial $2s$ electron in system A and its $2p$ state, as obtained at the Hartree-Fock level as a function of the distance R_0 . The vertical line is the distance at which the ICD takes place, R_{ICD} . It is seen to correspond to the maximum of the dipole transition moment.

produces a KER, which becomes almost constant [see Fig. 2(b)] as soon as system B is found again outside the diffuse electron cloud of system A . This is in contrast to the characteristic KER dependence of $1/R_0$ in the ICD process after ejection of the ICD electron into the continuum.

IV. CONCLUSIONS AND OUTLOOK

We have studied the interatomic Coulombic decay for the lithium dimer as a function of time by means of the electron and nuclear dynamics approach. The electronic structure of the lithium dimer is carried out at the level of time-dependent Hartree-Fock, which is equivalent to a random-phase approximation. Our results show that the initial $2s$ electronic state of the neutral atom is excited and ionized with the corresponding interatomic decay driven by a dipole-dipole interaction between the two atoms and falls into the well-analyzed class of ICD processes. Furthermore, we find that the ICD process occurs at the point of the strongest attractive dipole force in the dimer with a subsequent promotion to higher excited states followed by a Coulombic explosion. As shown by the dipole coupling term between the $2s$ and $2p$ states, the promotion starts at the point where it has the largest dipole transition moment. This distance is larger than the distance of closest

approach between the constituents of the dimer and corresponds to the point of maximal dipole force. Our results are consistent with the expression for the rate, Eq. (3), and the original picture of virtual photon exchange [40].

The present version of the END approach to ICD has two major shortcomings, the fingerprints of which can be seen in the results. In the ICD of the Li dimer, the $2s$ electron of $\text{Li}^+(1s2s)$ should relax and fill the $1s$ shell, while the excess energy is utilized to eject the $2s$ electron from the neighboring neutral $\text{Li}(1s^22s)$. This is a double excitation process not included in the one determinant description of the END used here. It is interesting to note that END describes the removal of the $2s$ electron from the neighbor. It does not, however, describe the filling of the $1s$ hole correctly. Due to the single determinant description for the electronic structure and the limited description of the continuum states by the END approach, the removed $2s$ electron is not ejected into a true continuum, but is rather excited into diffuse bound functions. On the other hand, by taking into account the time evolution

and the electron-nuclei coupling, the current END approach does provide a limited but interesting physical description of the ICD process driven by nuclear motion. The goal to describe ICD completely by END can be achieved by a multi-configuration extension of the method coupled to the nuclear dynamics and a better approximation of the continuum.

Note added in proof. Recently, we became aware of the work of Rander *et al.* [46] reporting an experiment on sodium dimer identifying an ICD process related to the one we discuss for lithium dimer.

ACKNOWLEDGMENTS

R.C.T. acknowledges support from Grants No. UNAM-DGAPA-PAPIIT IN-111-820, No. UNAM-DGAPA-PASPA, and No. LANCAD-UNAM-DGTIC-228, as well as the University of Heidelberg for its hospitality. L.S.C. gratefully acknowledges financial support by the European Research Council (Advanced Investigator Grant No. 692657).

-
- [1] L. S. Cederbaum, J. Zobeley, and F. Tarantelli, *Phys. Rev. Lett.* **79**, 4778 (1997).
- [2] S. Marburger, O. Kugeler, U. Hergenhahn, and T. Möller, *Phys. Rev. Lett.* **90**, 203401 (2003).
- [3] T. Jahnke, A. Czasch, M. S. Schöffler, S. Schössler, A. Knapp, M. Käs, J. Titze, C. Wimmer, K. Kreidi, R. E. Grisenti, A. Staudte, O. Jagutzki, U. Hergenhahn, H. Schmidt-Böcking, and R. Dörner, *Phys. Rev. Lett.* **93**, 163401 (2004).
- [4] T. Aoto, K. Ito, Y. Hikosaka, E. Shigemasa, F. Penet, and P. Lablanquie, *Phys. Rev. Lett.* **97**, 243401 (2006).
- [5] K. Kreidi, T. Jahnke, T. Weber, T. Havermeier, X. Liu, Y. Morisita, S. Schössler, L. P. H. Schmidt, M. Schöffler, M. Odenweller, N. Neumann, L. Foucar, J. Titze, B. Ulrich, F. Sturm, C. Stuck, R. Wallauer, S. Voss, I. Lauter, H. K. Kim, M. Rudloff, H. Fukuzawa, G. Prümper, N. Saito, K. Ueda, A. Czasch, O. Jagutzki, H. Schmidt-Böcking, S. Stoychev, P. V. Demekhin, and R. Dörner, *Phys. Rev. A* **78**, 043422 (2008).
- [6] M. Mucke, M. Braune, S. Barth, M. Frstel, T. Lischke, V. Ulrich, T. Arion, U. Becker, A. Bradshaw, and U. Hergenhahn, *Nat. Phys.* **6**, 143 (2010).
- [7] E. Aziz, N. Ottosson, M. Faubel, M. Faubel, I. V. Hertel, and B. Winter, *Nature (London)* **455**, 89 (2008).
- [8] T. Jahnke, H. Sann, T. Havermeier, K. Kreidi, C. Stuck, M. Meckel, M. Schöffler, N. Neumann, R. Wallauer, S. Voss, A. Czasch, O. Jagutzki, A. Malakzadeh, F. Afaneh, T. Weber, H. Schmidt-Böcking, and R. Dörner, *Nat. Phys.* **6**, 139 (2010).
- [9] N. Sisourat, N. Kryzhevoi, P. Kolorenč, S. Scheit, T. Jahnke, and L. S. Cederbaum, *Nat. Phys.* **6**, 508 (2010).
- [10] K. Gokhberg, P. Kolorenč, A. Kuleff, and L. S. Cederbaum, *Nature (London)* **505**, 661 (2014).
- [11] F. Trinter, M. Schöffler, H. Kim, F. P. Sturm, K. Cole, N. Neumann, A. Vredenburg, J. Williams, I. Bocharova, R. Guillemin, M. Simon, A. Belkacem, A. L. Landers, T. Weber, H. Schmidt-Böcking, R. Dörner, and T. Jahnke, *Nature (London)* **505**, 664 (2014).
- [12] P. O’Keeffe, E. Ripani, P. Bolognesi, M. Coreno, M. Devetta, C. Callegari, M. Di Fraia, K. C. Prince, R. Richter, M. Alagia, A. Kivimäki, and L. Avaldi, *J. Phys. Chem. Lett.* **4**, 1797 (2013).
- [13] M. Kimura, H. Fukuzawa, T. Tachibana, Y. Ito, S. Mondal, M. Okunishi, M. Schöffler, J. Williams, Y. Jiang, Y. Tamenori, N. Saito, and K. Ueda, *J. Phys. Chem. Lett.* **4**, 1838 (2013).
- [14] L. S. Cederbaum, *Phys. Rev. Lett.* **121**, 223001 (2018).
- [15] I. Cherkes and N. Moiseyev, *Phys. Rev. B* **83**, 113303 (2011).
- [16] A. Bande, K. Gokhberg, and L. S. Cederbaum, *J. Chem. Phys.* **135**, 144112 (2011).
- [17] A. Haller, D. Peláez, and A. Bande, *J. Phys. Chem. C* **123**, 14754 (2019).
- [18] H. Agueny, M. Pesche, B. Lutet-Toti, T. Miteva, A. Molle, J. Caillat, and N. Sisourat, *Phys. Rev. B* **101**, 195431 (2020).
- [19] V. Averbukh and L. S. Cederbaum, *J. Chem. Phys.* **123**, 204107 (2005).
- [20] S. Kopelke, K. Gokhberg, V. Averbukh, F. Tarantelli, and L. S. Cederbaum, *J. Chem. Phys.* **134**, 094107 (2011).
- [21] N. Moiseyev, *Isr. J. Chem.* **31**, 311 (1991).
- [22] M. K. Mishra and M. N. Medikeri, *Adv. Quantum Chem.* **27**, 223 (1996).
- [23] R. Santra, L. Cederbaum, and H.-D. Meyer, *Chem. Phys. Lett.* **303**, 413 (1999).
- [24] N. Vaval and L. S. Cederbaum, *J. Chem. Phys.* **126**, 164110 (2007).
- [25] A. Ghosh, S. Pal, and N. Vaval, *Mol. Phys.* **112**, 669 (2014).
- [26] R. Santra, J. Zobeley, L. S. Cederbaum, and N. Moiseyev, *Phys. Rev. Lett.* **85**, 4490 (2000).
- [27] A. Landau, A. Ben-Asher, K. Gokhberg, L. S. Cederbaum, and N. Moiseyev, *J. Chem. Phys.* **152**, 184303 (2020).
- [28] G. Jabbari, K. Sadri, L. S. Cederbaum, and K. Gokhberg, *J. Chem. Phys.* **144**, 164307 (2016).
- [29] E. Deumens, A. Diz, R. Longo, and Y. Öhrn, *Rev. Mod. Phys.* **66**, 917 (1994).
- [30] R. Cabrera-Trujillo, J. R. Sabin, Y. Öhrn, and E. Deumens, *Phys. Rev. A* **61**, 032719 (2000).

- [31] R. Cabrera-Trujillo, J. R. Sabin, Y. Öhrn, and E. Deumens, *Phys. Rev. Lett.* **84**, 5300 (2000).
- [32] N. Stolterfoht, R. Cabrera-Trujillo, Y. Öhrn, E. Deumens, R. Hoekstra, and J. R. Sabin, *Phys. Rev. Lett.* **99**, 103201 (2007).
- [33] R. Cabrera-Trujillo, Y. Öhrn, E. Deumens, and J. R. Sabin, *J. Chem. Phys.* **116**, 2783 (2002).
- [34] B. J. Killian, R. Cabrera-Trujillo, E. Deumens, and Y. Öhrn, *J. Phys. B* **37**, 4733 (2004).
- [35] R. Cabrera-Trujillo, E. Deumens, Y. Öhrn, O. Quinet, J. R. Sabin, and N. Stolterfoht, *Phys. Rev. A* **75**, 052702 (2007).
- [36] R. Cabrera-Trujillo, Y. Öhrn, E. Deumens, and J. R. Sabin, *J. Phys. Chem. A* **108**, 8935 (2004).
- [37] R. Cabrera-Trujillo, Y. Öhrn, E. Deumens, J. R. Sabin, and B. G. Lindsay, *Phys. Rev. A* **70**, 042705 (2004).
- [38] R. Santra and L. S. Cederbaum, *Phys. Rep.* **368**, 1 (2002).
- [39] A. I. Kuleff and L. S. Cederbaum, *Phys. Rev. Lett.* **98**, 083201 (2007).
- [40] V. Averbukh, I. B. Müller, and L. S. Cederbaum, *Phys. Rev. Lett.* **93**, 263002 (2004).
- [41] V. Stumpf, K. Gokhberg, and L. Cederbaum, *Nat. Chem.* **8**, 237 (2016).
- [42] E. Deumens, T. Helgaker, A. Diz, H. Taylor, J. Oreiro, B. Mogensen, J. A. Morales, M. C. Neto, R. Cabrera-Trujillo, and D. Jacquemin, *ENDyne version 2.8 Software for Electron Nuclear Dynamics*, Quantum Theory Project, University of Florida, Gainesville, FL, 2000.
- [43] T. H. Dunning, *J. Chem. Phys.* **90**, 1007 (1989).
- [44] R. C. Raffanetti, *J. Chem. Phys.* **59**, 5936 (1973).
- [45] R. D. Bardo, Even-tempered Gaussian atomic orbital bases in quantum chemistry: Ab initio calculations on atoms hydrogen through krypton and on molecules containing carbon, hydrogen, and oxygen, Master's thesis, Iowa State University, 1973.
- [46] T. Rander, J. Schulz, M. Huttula, A. Mäkinen, M. Tchapyguine, S. Svensson, G. Öhrwall, O. Björneholm, S. Aksela, and H. Aksela, *Phys. Rev. A* **75**, 032510 (2007).